ORIGINAL ARTICLE

An improved cutting force prediction model in the milling process with a multi-blade face milling cutter based on FEM and NURBS

Sijie Cai[1] · Bin Yao[1] · Wei Feng[2] · Zhiqin Cai[1]

Abstract
Multi-blade face milling cutters are widely used in the finish machining of mechanical parts. The cutting force in the milling process is a crucial factor that promotes the chatter of the machine spindles, which can be used to predict the machined surface roughness. In this paper, a novel cutting force prediction model based on non-uniform rational basis splines (NURBS) and finite element method (FEM) is proposed. Single blade cutting forces under different parameters are simulated by FEM, and a cutting force model of the single blade is established by the NURBS interpolation method. Then, combined with the tool tip motion model, the cutting force of the multi-blade face milling cutter can be predicted. To verify the correctness of the cutting force predicted by the proposed method, the common coefficient-based cutting force mathematical prediction method is utilized as benchmark for comparison with the predicted results. The accuracy is verified by comparison with experimental data. According to the collected experimental data, the proposed model is proved to be an accurate and efficient method to predict the cutting force of the multi-blade face milling cutter in the milling process.

Keywords Multi-blade face milling cutter · NURBS · FEM · Cutting force model · Tool tip motion model

1 Introduction

Multi-blade face milling cutters are widely used in the face milling process. In order to improve the accuracy of surface finishing machining [1], the cutting force balance and the chatter stability of the cutter must be optimized by proposing a proper scheme for the geometry of the cutter and a reasonable distribution of the blades in the cutter [2, 3]. Cutting force also can be used to calculate the wear extent of the cutter [4, 5]. The cutting force model of the milling process should be established to provide a standard for the design of multi-blade face milling cutters.

✉ Bin Yao
yaobin@xmu.edu.cn

Sijie Cai
xmucsj@163.com

1 Department of Mechanical and Electrical Engineering, Xiamen University, Xiang'an District, Xiamen 361106, Fujian Province, China

2 School of Mechanical and Electronic Engineering, Henan University of Technology, High-tech District, 450001, Zhengzhou 450001, Henan Province, China

To establish the cutting force model, current methods can be classified as either a finite element method (FEM) or a mathematical model with several cutting force coefficients identified in the cutting experiment. Based on the radial, axial, and tangential shear coefficients and the edge coefficients identified in the cutting force experiment, Engin and Altintas [6] established the cutting force model and predicted the cutting force. According to the transfer function model of the force and vibration of the spindle and the cutting force coefficients, Altintas predicted the chatter stability lobes, the spindle chatter, and the machined surface geometry. Based on the method of the cutting force coefficients mentioned above, Liu [7] established the down-milling force model and up-milling force model and analyzed the theory of the cutting force model. In that article, the cutting force in the peripheral milling of different parameters of the cutter was simulated and compared. The tool path in the face milling process and the corresponding cutting force in various CAD-CAM systems was researched by Tapoglou and Aristomen [8]. This research can provide a more accurate motion model with which to calculate the chip thickness for the research of face milling cutting force. It also can predict the surface topography of the workpiece accurately. For the cutting force coefficients identification method, besides the average cutting force model and the transient cutting force model, Ghorbani identified the specific cutting force coefficients based on the artificial neural network with the cutting

parameters, such as cutting speed, feed per tooth, and depth of cut [9]. Yoon also simulated the cutting force based on the cutting force coefficients by visual C++ and MATLAB and compared simulated cutting force and experimental cutting force with different cutting parameters [10].

The method of cutting force coefficient identification can also be used in the turning. Jian established the cutting force model based on the turning power [11]. This method measures turning power in the cutting process and identifies the cutting force coefficients based on the power curve. Response surface methodology is another common method used in the cutting force prediction of turning. Bouacha used response surface methodology to model the cutting parameter of the cutting force and surface roughness of turning of ANSI52100 bearing steel based on the experimental data [12]. D.I. Lalwani put forward a linear model of the cutting force and a nonlinear model for the surface roughness to reduce the error of the response surface model in range of 55–93 m/min of cutting feed speed in finish hard turning of the MDN250 steel [13]. Moreover, a neural network is also used in the cutting force prediction or surface roughness prediction. For example, the turning cutting force based on ANFIS was established by Jain and Raj [14]. ANFIS is the adaptive neuro-fuzzy inference system. It is a combination of fuzzy and neural networks. Neural networks are trained by data, while fuzzy logic is followed by rules in linguistic form like IF–THEN rules. They can express the cutting force of the blade infinitesimal as a complex non-linear model. However, to improve the accuracy of the cutting force model, many experiments or simulations with different cutting parameters must be conducted to provide data to establish the cutting force model. In addition, Sharma [15] used the artificial neural network model to predict the cutting force and surface roughness with parameters such as approaching angle, speed, feed, and depth of cut.

To predict the cutting force with vibration, an improved mathematical model of cutting force coefficients was proposed by Yao and Wu [16], which took the mass matrix, damping matrix, and stiffness matrix of cutters into account, and the cutting coefficient model with the cutting axial depth is proposed to improve the cutting force model. Li [17] devised a method that combines the stability model of the spindle in the cutting process, the chatter model of the cutter tip associated with the speed of the spindle, and the cutting force identification method to predict the accurate cutting force. Yu [18] also researched the spindle chatter based on the cutting force coefficient and studied the vibration of the cutting force and the cutting force coefficient in different cutting parameters. Wan put forward a general cutting force method of flexible end milling. The deflection of the workpiece was calculated to modify the entry angle and the instantaneous uncut chip thickness. Based on the cutting coefficients and the modified instantaneous uncut chip thickness, the accurate cutting force can be calculated [19].

In most of the introduced methods, the cutting force model is established based on the cutting coefficients. Since the cutting coefficients are generally extracted from the cutting force measured in the experiments, a force measuring system is necessary to predict the cutting force model. Furthermore, the cutting force of multi-blade face milling cutters with large diameter can hardly be simulated by the FEM due to the large amount of calculation required by the FEM.

In this paper, we present a novel cutting force prediction method without a force measuring system that is based on non-uniform rational basis splines (NURBS) and the FEM. The milling process is decomposed to simulate the cutting force in this method. This will increase the efficiency of the cutting force prediction and reduce the amount of calculation. NURBS is widely used in complex surface molding [20], but it can also be used to establish other models. Chen [21] used NURBS to solve the chaotic time series and provided a time factor method to solve the disadvantage of the NURBS method, which does not have a time factor.

The simulation process of the proposed method, which is shown in Fig. 1, has four main steps:

1. The cutting force model for a single blade should be established first. The corresponding parameters of the material and the friction coefficients should be tested under different undeformed chip thicknesses and axial cutting depths.
2. Based on the cutting force simulation data, the cutting force model can be established by the interpolated NURBS.
3. According to the tool path model and the single blade cutting force model, the axial, radial, and tangential cutting forces of each blade in the milling process can be calculated.
4. The cutting forces of multiple blades can be simulated via coordinate transformation and tool superposition.

Subsequently, the proposed simulation process for cutting force, established by several transient cutting forces based on the interpolated NURBS, can reduce the amount of calculation required by FEM. The cutting force experiments are not necessary to the cutting force model because the transient cutting force samples of the blade are obtained by simulation.

2 The motion model for the cutting process

To simulate the cutting forces of the blades, the path of each blade should be calculated. The coordinate system for blade O′-uvw and the coordinate system for cutter O-XYZ are established as shown in Fig. 2 [4]. The geometry of the tool is regarded as a rectangular solid. The transformation model

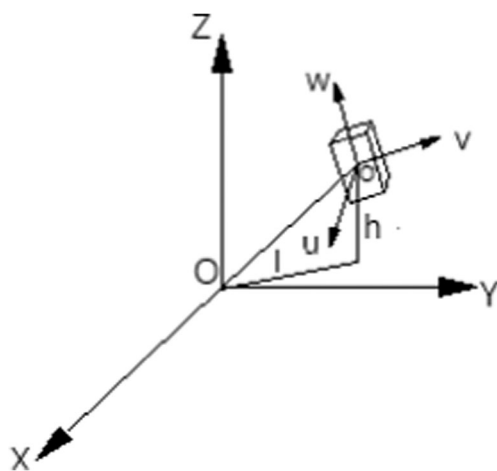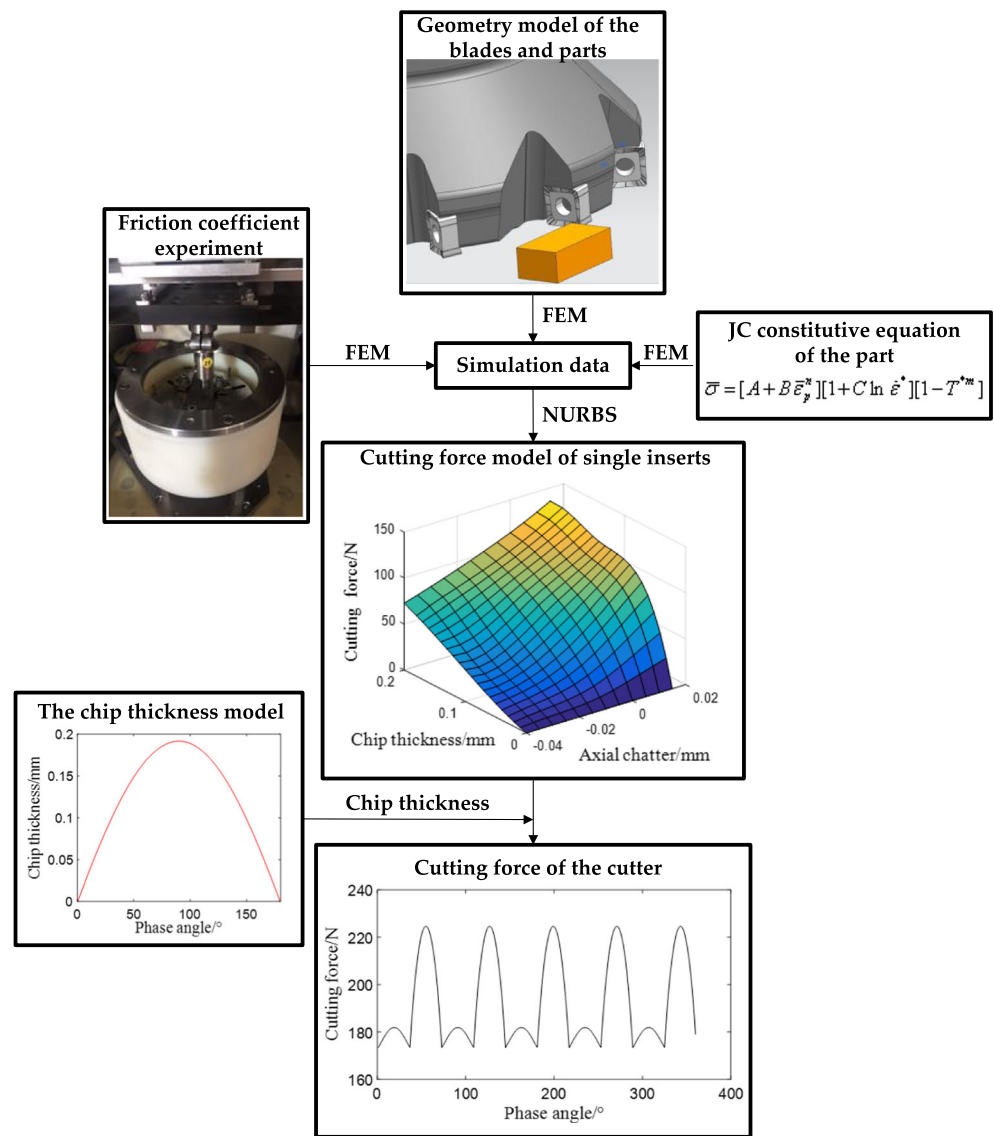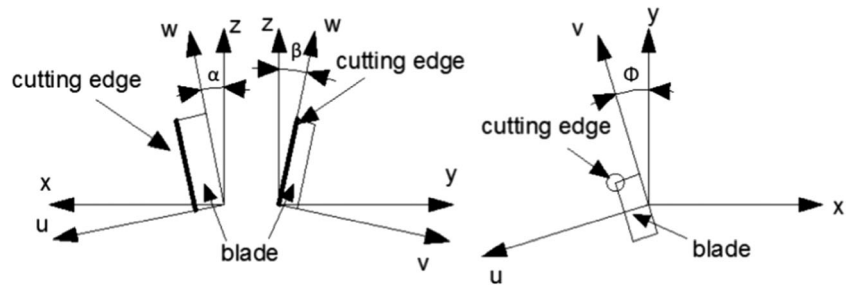**Fig. 1** The process chart of cutting force simulation

Geometry model of the blades and parts

Friction coefficient experiment

FEM

FEM Simulation data FEM

JC constitutive equation of the part

$$\bar{\sigma} = [A + B\bar{\varepsilon}_p^n][1 + C\ln\dot{\bar{\varepsilon}}^*][1 - T^{*m}]$$

NURBS

Cutting force model of single inserts

The chip thickness model

Chip thickness

Cutting force of the cutter

Fig. 2 The relationship between cutter's coordinate system and blade's coordinate system

can be described with three rotation matrices and a translation matrix as expressed in Eq. 1, where T_α, T_β, and T_ϕ represent the rotation matrices, and Tp represents the translation matrix.

$$\begin{bmatrix} x \\ y \\ z \end{bmatrix} = T_\alpha T_\beta T_\varphi \begin{bmatrix} u \\ v \\ w \end{bmatrix} + T_P \tag{1}$$

The blade is rotated by $\varphi/\alpha/\beta$ around the $x/y/z$-axis as shown in Fig. 3. The space position matrices of the blades, T_α, T_β, T_ϕ, and T_P, can be expressed by Eqs. 2 and 3. The parameter h is the distance between the blade center and the O-XY plane. Based on these matrices, the blade can be positioned in the coordinate system of the workpiece. Additionally, the geometry model of the blade and the workpiece can be established by this model.

**Fig. 3** The rotation angle of the inserted coordinate system

$$T_\alpha = \begin{bmatrix} sin\alpha & 0 & cos\alpha \\ 0 & 1 & 0 \\ cos\alpha & 0 & -sin\alpha \end{bmatrix} T_\beta$$

$$= \begin{bmatrix} 1 & 0 & 0 \\ 0 & cos\beta & sin\beta \\ 0 & -sin\beta & cos\beta \end{bmatrix} T_\varphi = \begin{bmatrix} -cos\varphi & -sin\varphi & 0 \\ -sin\varphi & cos\varphi & 0 \\ 0 & 0 & 1 \end{bmatrix} \quad (2)$$

$$T_p = \begin{bmatrix} lsin\theta \\ lcos\theta \\ h \end{bmatrix} \quad (3)$$

Next, the path of the blade's tip should be calculated. The path of the adjacent blades can be expressed by Eq. 4. In Eq. 4, r is the radius of the cutter, w is the angular velocity of the cutter, θ_0 is the initial phase angle of the tool tip, and f is the feed speed. As shown in Fig. 4, the cutter moves along the x direction. When the tool tip is located at the y-axis, the rotation phase angle, θ, is defined as 0°. The rotation direction of the cutter is defined as the positive direction of the phase angle.

$$\begin{cases} x = rsin(wt + \theta_0) \\ y = rcos(wt + \theta_0) + ft \\ \theta = wt + \theta_0 \end{cases} \quad (4)$$

Based on the path, the model of the undeformed chip thickness and the rotated angle can be established by two methods: (1) The undeformed chip thickness can be expressed by Eq. 5,
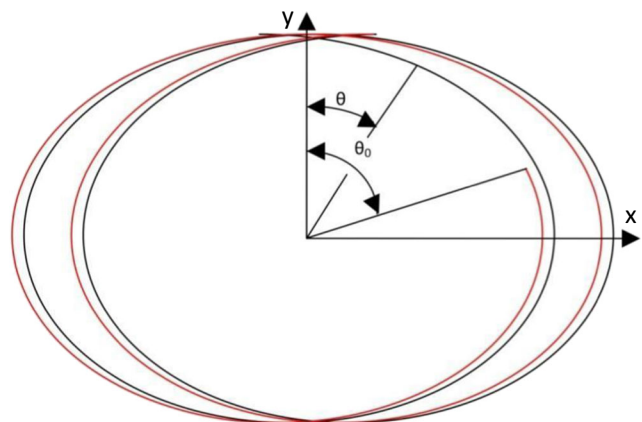
Fig. 4 The path of the adjacent blade's tip

and (2) the undeformed chip thickness can be defined as the distance of two traces in the same phase angle θ.

$$a_{pd} = f_t sin\theta \quad (5)$$

3 The blades cutting force simulation by FEM

The cutting force prediction method based on NURBS and the FEM can be used to establish the relationship of cutting force and cutting parameters, such as the axial cutting depth and the undeformed chip thickness or the axial vibration and the undeformed chip thickness.

To establish the cutting force model about axial cutting depth and undeformed chip thickness, the geometry model of the blade and the parts can be described as shown in Fig. 5(a). The blade tip is tightly attached to the machined surface.

To establish the cutting force model about the vibration amplitude, the geometry model must be built as shown in Fig. 5(b). The blade tip is far away from the machined surface for random vibration. When the blade tip is above the machined surface, the vibration amplitude is defined as positive.

Several geometry models for different undeformed chip thicknesses and vibration amplitudes are established as shown in Fig. 6. For convenience, only the region of contact between the blade tip and workpiece is isolated from the cutting system and studied. Thus, a more suitable grid can be chosen to describe the contact line between the blade and the workpiece, and the transient force can be simulated with higher accuracy.

Besides the geometry model, the friction coefficient and the material parameters should be measured to simulate the transient cutting force. This article focuses on the cutting process of the cemented carbide blade and the HT250 workpiece. The Johnson-Cook constitutive equation is used to describe the material property of the HT250, and the corresponding constitutive coefficients, shown in Table 1, are obtained from other articles [22].

The coefficient of shear friction between the cemented carbide and the HT250 is measured by the friction and wear tester as shown in Fig. 7(a). An ETR UMT-2M tribometer is used to measure the shear friction coefficient. This tribometer

Fig. 5 The geometry model of different research purposes. (**a**) The geometry model to research the relationship between the cutting force and the axial cutting depth and the undeformed chip thickness. (**b**) The geometry model to research the relationship between the cutting force and the vibration and the undeformed chip thickness
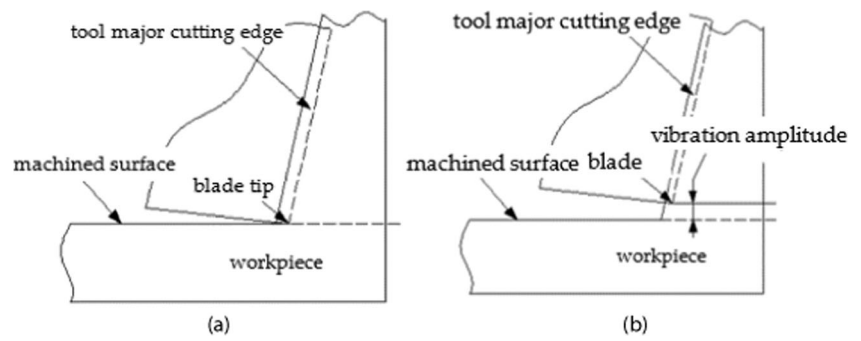
comprises a measurement system and a turntable. The pressure head is clamped onto the measurement system and the workpiece onto the turntable. The pressure between the pressure head and the workpiece and the rotation speed of the workpiece is set, and then the friction force can be measured and the shear friction coefficients calculated. In the experiment, the pressure head made by the cemented carbide is fixed, and the disk made by HT250 is installed in the clamp. When the pressure head exerts a 20 N force on the disk, the disk rotates at 600 rev/min, and the coefficient of shear friction can be measured. The measured data are shown in Fig. 7(b).

Based on the model and parameters, which are mentioned above, several transient cutting forces can be simulated. However, the transient force model should be generated in order to calculate the cutting force or simulate the force with the enhancement of vibration in the milling process.

4 The single insert cutting force model established by NURBS

As the cutting force of each insert increases with the axial cutting depth and undeformed chip thickness, the bicubic B-spline surface interpolation can be applied to generate the cutting force model. The control surface of B-spline surface interpolation is composed of the control point and the primary function. Its equation can be expressed as Eq. 6.
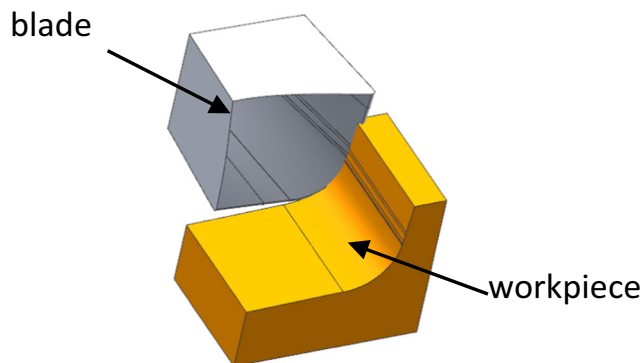
Fig. 6 The geometry model of the blade and the workpiece

$$F(u,v) = \sum_{i=0}^{m}\sum_{j=0}^{n} N_i(u)G_j(v)\mathbf{P_{ij}} \qquad (6)$$

In this equation, N_i and G_j are the primary functions of the u direction and v direction, respectively, and P_{ij} is the control point. The parameters i and j express the sequence number of the B-spline curves, which combine the whole B-spline surface. To ensure the continuity of the surface and its first derivative, the primary function can be expressed by Eq. 7.

$$N_{i,0}(u) = \begin{cases} 1, u_i \leq u < u_{i+1} \\ 0 \end{cases}$$
$$N_{i,p}(u) = \frac{u-u_i}{u_{i+p}-u_i}N_{i,p-1}(u) + \frac{u_{i+p+1}-u}{u_{i+p+1}-u_{i+1}}N_{i+1,p-1}(u) \qquad (7)$$

In Eq. 7, N is the primary function, i is the sequence number of the B-spline curve, and p is the order number of the primary function. To calculate the primary function, the low-order primary function must be calculated first. Based on the data of the low-order primary function, the primary function of the B-spline surface can be calculated by the iteration method.

The simulation data is made up of points on the B-spline surface. To calculate the whole model, the control points and the primary function should be calculated first. The whole surface is composed of several cubic B-spline surfaces. Therefore, the simulation cutting parameters require specific regulation. As shown in Fig. 8, U is the axial cutting depth and V is the undeformed chip thickness.

The simulation data are located at the corners or the borders of the B-spline surface or in the surface. When dividing the border of the surface, the border A in the u direction can be divided into n curves and the border B in the v direction can be divided into m curves. Additionally, p is the order number of the B-spline, and h, which can be expressed as Eq. 8, is the

Table 1 The constitutive coefficients of HT250

A	B	C	D_0	E	n	m	ε_0	T_{room}	T_{melt}
573	380	0.034	1	1	0.17	1.12	1	20	1350

Fig. 7 Tribometer and the curve of shear friction

(a)

(b)
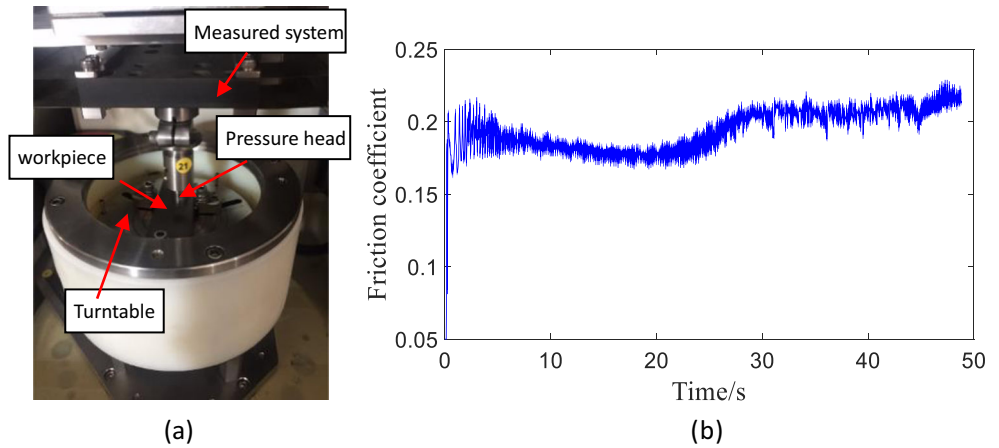
number of control points in the border A. The parameter t is the number of control points in the border B, and the parameter k, which can be expressed as Eq. 9, expresses the number of control points in the whole B-spline surface.

$$h = n \times (p-1) + 1 \qquad (8)$$

$$k = h \times t \qquad (9)$$

According to Eqs. 8 and 9, the parameters of cutting simulation can be ensured based on the scale of the cutting parameters researched. The more simulation data there are, the higher the accuracy of the cutting force model. In the cutting force model, u expresses the axial cutting depth or the axial vibration, and v is the undeformed chip thickness. To establish the cutting force model, according to the cutting parameter, the primary functions in the u direction and v direction can be solved based on Eq. 7, and the cutting force can be calculated by Eq. 10.

Fig. 8 The cutting force model

$$\begin{bmatrix} N_1(u_1) & N_2(u_1) & \ldots & N_n(u_1) \\ N_1(u_2) & N_2(u_2) & \ldots & N_n(u_2) \\ \ldots & \ldots & \ldots & \ldots \\ N_1(u_n) & N_2(u_n) & \ldots & N_n(u_n) \end{bmatrix} \qquad (10)$$

$$\left(\begin{bmatrix} G_1(v_1) & G_2(v_1) & \ldots & G_t(v_1) \\ G_1(v_2) & G_2(v_2) & \ldots & G_t(v_2) \\ \ldots & \ldots & \ldots & \ldots \\ G_1(v_t) & G_2(v_t) & \ldots & G_t(v_t) \end{bmatrix} \begin{bmatrix} P_{11} & P_{12} & \ldots & P_{1t} \\ P_{21} & P_{22} & \ldots & P_{2t} \\ \ldots & \ldots & \ldots & \ldots \\ P_{n1} & P_{n2} & \ldots & P_{nt} \end{bmatrix}^T \right)^T$$

$$= \begin{bmatrix} F_{11} & F_{12} & \ldots & F_{1t} \\ F_{21} & F_{22} & \ldots & F_{2t} \\ \ldots & \ldots & \ldots & \ldots \\ F_{n1} & F_{n2} & \ldots & F_{nt} \end{bmatrix}$$

In Eq. 10, N is the primary function in the direction of the axial cutting depth, G is the primary function in the direction of the undeformed chip thickness, F is the transient simulated cutting force based on the cutting parameters, and P is the matrix of control points. Based on the calculated primary function and the simulation data, the control points can be calculated and the cutting force model of the blade is established.
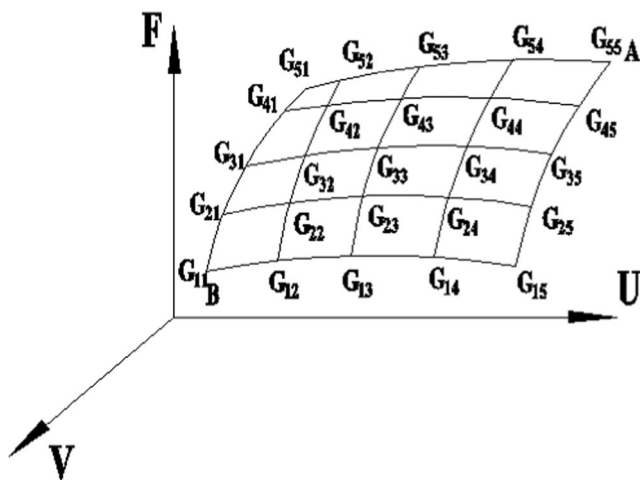
5 The cutting force of the whole cutter prediction

According to the cutting force model of the blades and the track of the blade, the cutting force of the whole cutter can be generated. The initial phase angle, Φ_{st}, and the ending phase angle, Φ_{ex}, can be expressed by Eq. 11. As shown in Fig. 9, these two parameters express the phase angle beginning cutting and finishing cutting. The range of the phase angle of the cutter directly involved in the milling process is defined by these parameters.

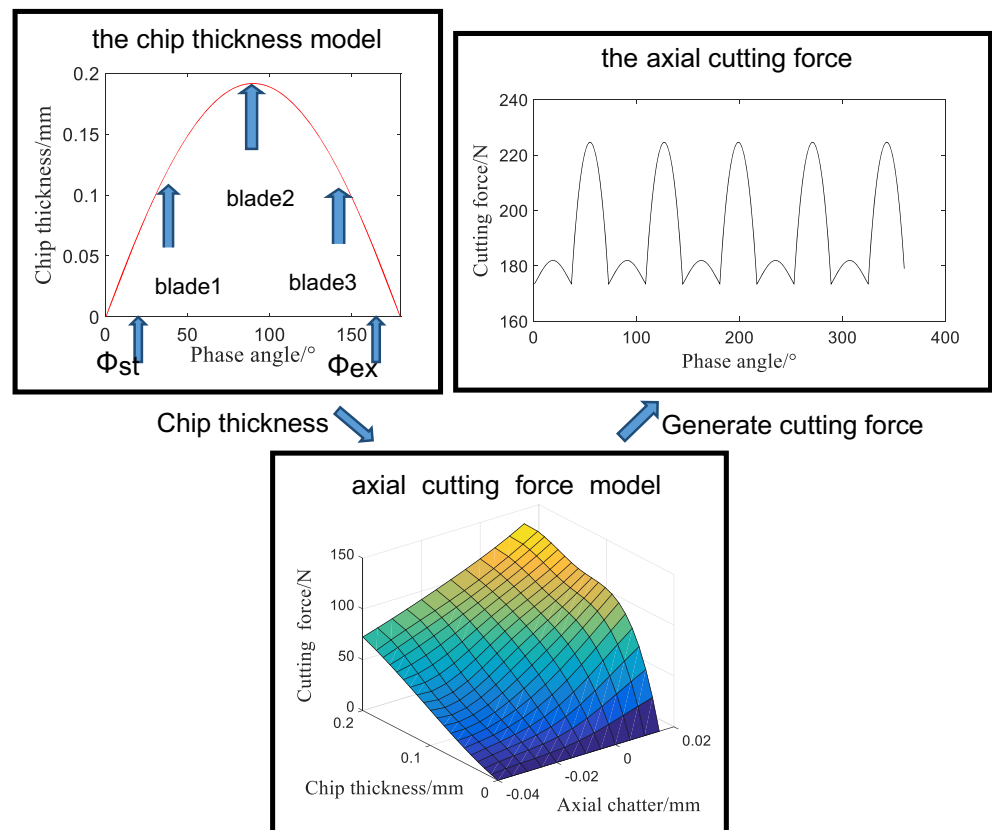**Fig. 9** The initial phase angle and ending phase angle
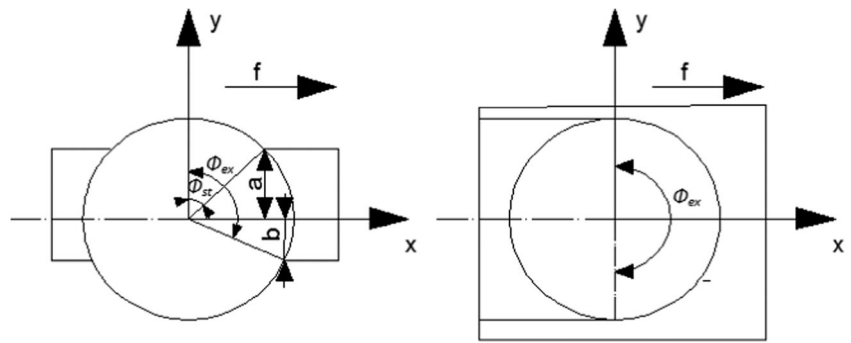
$$\begin{cases} \phi_{st} = \dfrac{\pi}{2} - \arcsin\dfrac{a}{R}\,(a < R) \\ \phi_{st} = 0\,(a \geq R) \\ \phi_{ex} = \dfrac{\pi}{2} + \arcsin\dfrac{b}{R}\,(b < R) \\ \phi_{ex} = \pi\,(b \geq R) \end{cases} \tag{11}$$

In Eq. 11, if the cutting initial point is in the first quadrant, the parameter a is positive. If the cutting ending point is in the fourth quadrant, the parameter b is positive. As shown in Figs. 10 and 11, the undeformed chip thickness can be calculated by the rotated phase angle of the blades. Based on the undeformed chip thickness and the axial cutting depth, the transient cutting force of the
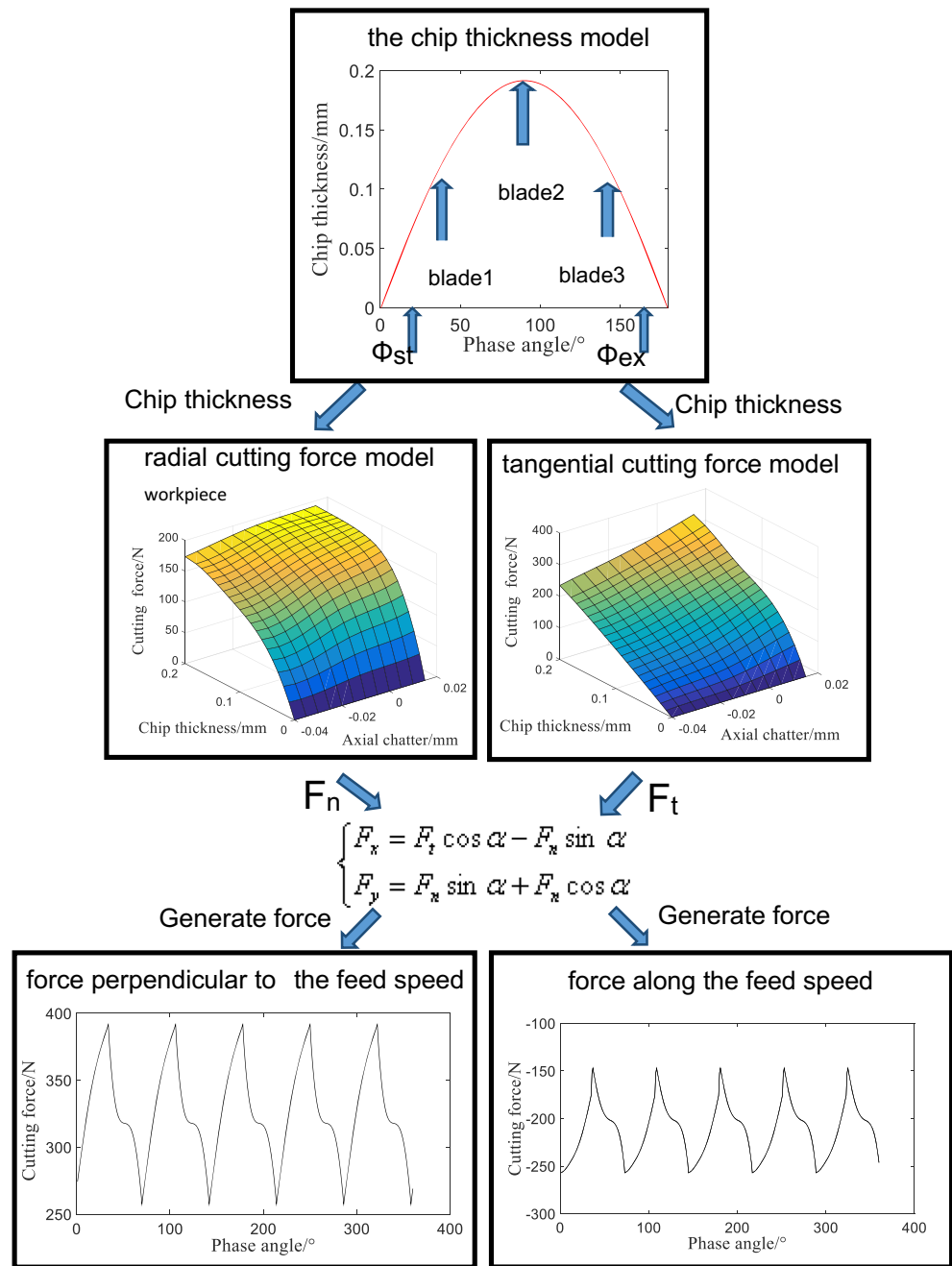
blades can be calculated. However, the force model of the blades can only describe the relationship between the cutting parameters and the tangential force, radial force, and axial force.

Since the direction of the force of each insert is different, in order to calculate the force of the whole cutter, the force of each insert must be separated into components aligned with the feed direction, the axial direction of the cutter, and the direction perpendicular to these two directions. Then, the force of the whole cutter can be calculated. Considering the change of the undeformed chip thickness of the whole track, the force of the cutter in the cutting process can be generated as Figs. 10 and 11 show.

Fig. 10 The generation of the axial force of the cutter

Fig. 11 The generation of the force of the cutter along the feed direction

The chip thickness model

radial cutting force model

tangential cutting force model

$$\begin{cases} F_x = F_t \cos \alpha - F_n \sin \alpha \\ F_y = F_n \sin \alpha + F_n \cos \alpha \end{cases}$$

force perpendicular to the feed speed

force along the feed speed

6 The comparison of the theory models and experiment

To validate the precision of the cutting force prediction model based on NURBS, the cutting force coefficient identification model and the experiment data are compared with the prediction model. The cutting force of the milling process with a five-blade ending milling cutter is researched. The spindle speed is 800 rev/min, the feed speed is 400 mm/min, and the cutting depth is 1.5 mm. First, the motion model of the blade tips is established by calculating the distance of the adjacent tool tip in the same phase angle as mentioned in Sect. 2.

Several undeformed chip thicknesses with different phase angles are shown in Table 2.

After calculating the motion model, the parameter scales of the cutting force model can be ensured based on the undeformed chip thickness and the axial cutting depth. Then, the geometry model of the blade and the part is established. In this study, the relationship of the cutting force and the vibration and the undeformed chip thickness is established. The geometry model is established as shown in Fig. 5(b). Based on this geometry model, the cutting force is calculated by the FEM. The parameters of the workpiece material constitutive equations and the friction coefficient are shown in Sect. 3.

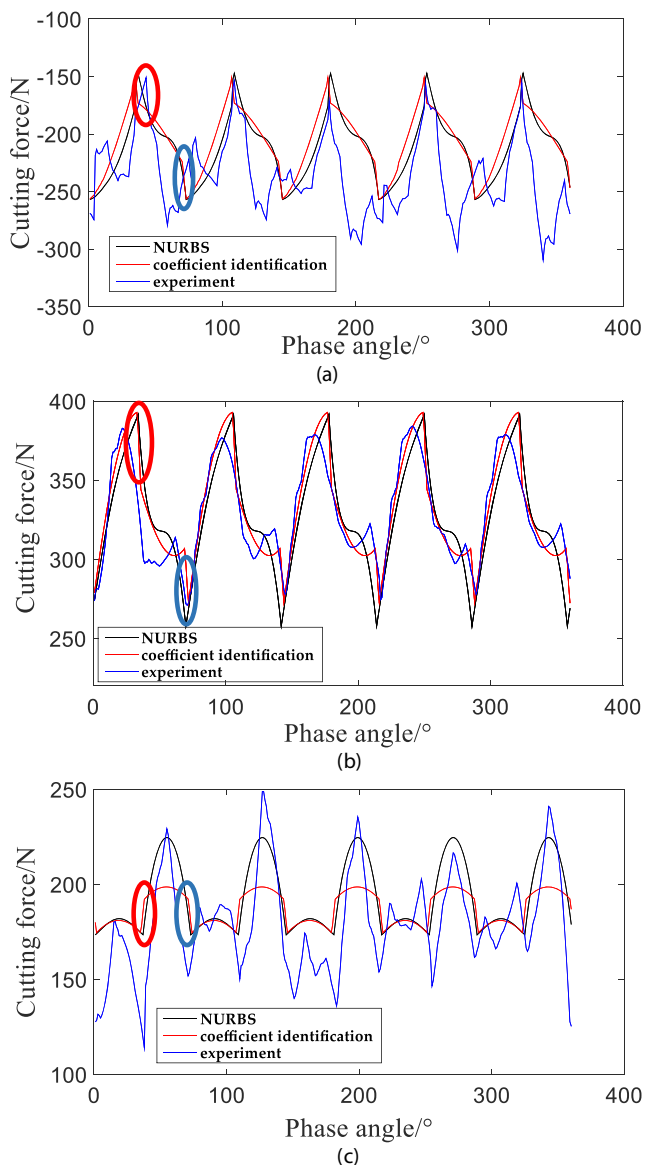**Table 2** Several phase angles and the undeformed chip thickness

Phase angle	0	18	36	54	72
Undeformed chip thickness (mm)	0	0.0592	0.1146	0.1587	0.1871
Phase angle	90	108	126	144	162
Undeformed chip thickness (mm)	0.2	0.1871	0.1587	0.1146	0.0592

Fig. 12 Cutting force model of the blade. (**a**) Radial force. (**b**) Tangential force. (**c**) Axial force

(a)

(b)

(c)
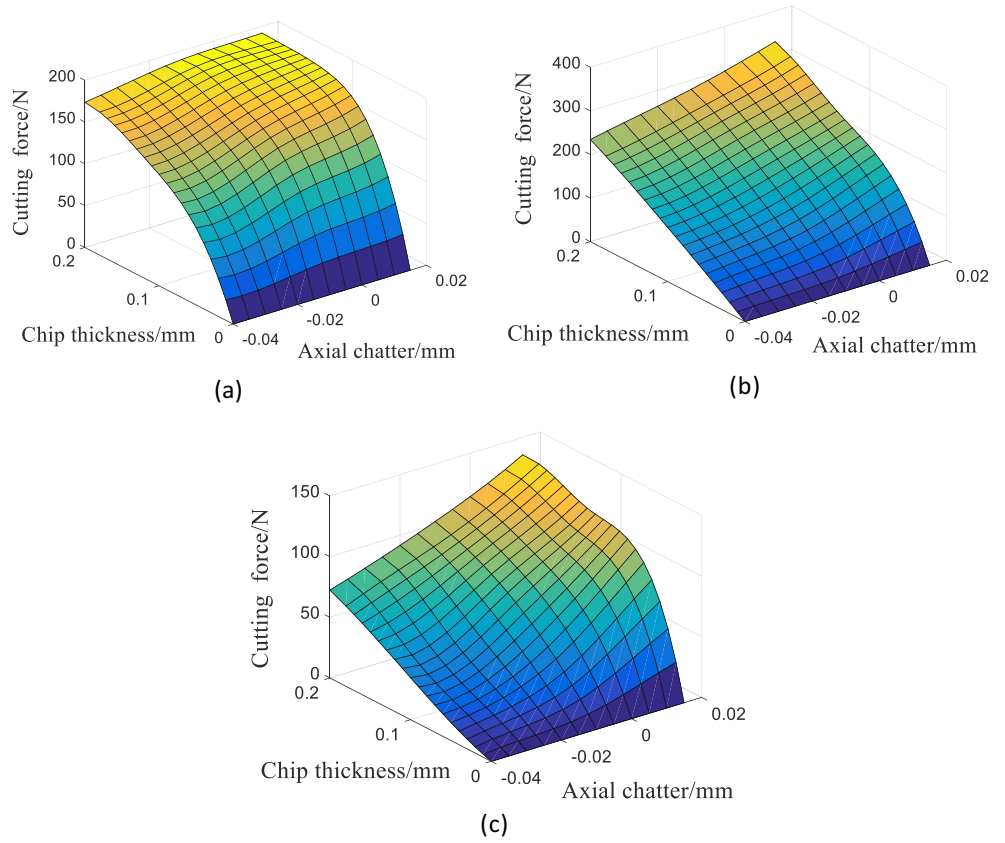
Fig. 13 The cutting force experiment

Fig. 14 The cutting force comparison. (**a**) Cutting force along the feed speed. (**b**) Cutting force perpendicular to the feed speed. (**c**) Cutting force along axial direction of the cutter

According to the simulation data, the cutting force model can be generated by NURBS. The cutting force model of the blade is expressed in Fig. 12. As Fig. 13 shows, the tangential cutting force model, axial cutting force model, and the radial cutting force model can be established based on this data.

By combining the cutting force model and the motion model as shown in Sect. 5, the final cutting force, which is named NURBS of the whole cutter, can be generated.

To compare the precision of these methods, the cutting force coefficient identification algorithm [1] is used to generate the cutting force, which is named coefficient identification for the same cutting parameters.

To verify the predictions of the proposed cutting force model, an experiment with the same cutting parameters is conducted using the DMG machine and the 9257B KISTLER cutting force measurement instrument as Fig. 13 shows. The results of the experiment are shown in Fig. 14.

Figure 14(a) is the comparison of the radial cutting force between the cutting force model based on NURBS and the FEM, the cutting force model based on coefficients identification, and the experimental cutting force. Figure 14(b) is the comparison of the tangential cutting force. Figure 14(c) is the comparison of the axial cutting force. As Fig. 14 shows, the cutting force generated by NURBS and the FEM is similar to the cutting force generated by the method of coefficient identification. Along the axial direction of the cutter, the accuracy of the cutting force is even higher than the cutting force generated by the average cutting force coefficients. In addition, the process of the blades' pitch into and cut out can be found easily in Fig. 14. Since the cutter is a five-blade cutter, a blade will cut out the workpiece in the half of the cutting force cycle, and at the end of the cutting force cycle, another blade will pitch into the workpiece as shown in Fig. 15. In the red circle, the cutting force of the process of the blade cut into the workpiece is expressed. In the blue circle, the cutting force of the process of another blade cut out of the workpiece is expressed. Moreover, the cutting force in the process of the blade pitching into the workpiece or cutting out of the workpiece is also similar to the cutting force identification method. In Fig.

Fig. 15 The pitching-in process and the cutting-out process
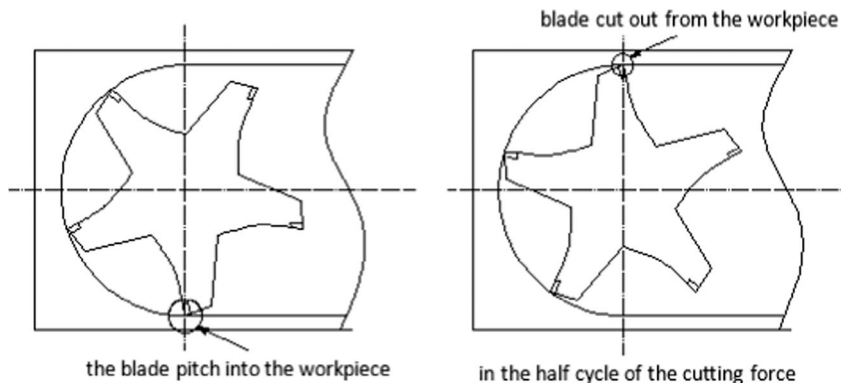
(a)   (b)
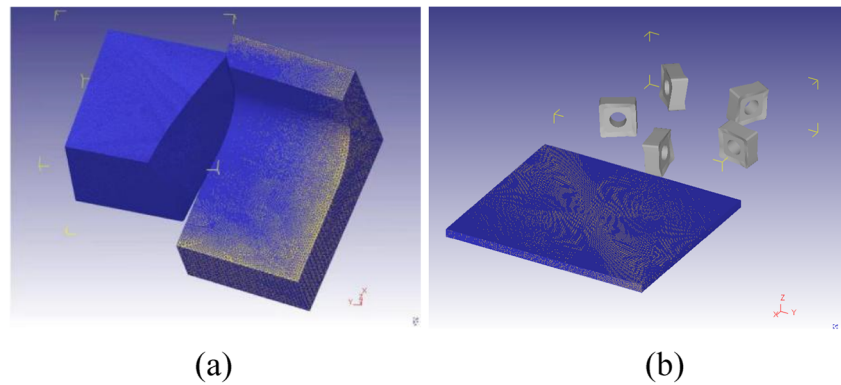
14(b), the experimental cutting force fluctuates less, which is similar to the cutting force generated by NURBS and the FEM. However, the experimental cutting force along the axial direction of the cutter and the experimental cutting force along the feed speed have a lager fluctuation. Causes of fluctuations in experimental forces will be proposed in Sect. 7.

7 Discussion

To compare the efficiency of the cutting force model based on NURBS and the cutting force simulation by the FEM, the simulation of the cutting force of the whole cutter and the simulation of the transient cutting force of the tool tip were carried out as Fig. 16 shows. The number of grids and the tool tip rotation angle during the whole process of simulation are provided in Table 3.

As Table 3 shows, although several simulations are needed to generate the model in the method based on NURBS, each workpiece only requires simulation of the process in which the tool tip moves 1°, and several simulations can be achieved at the same time with one computer. Additionally, the number of grids of the simulation of NURBS is less than that of the FEM. Hence, the efficiency of the NURBS method is higher than the efficiency of the FEM.
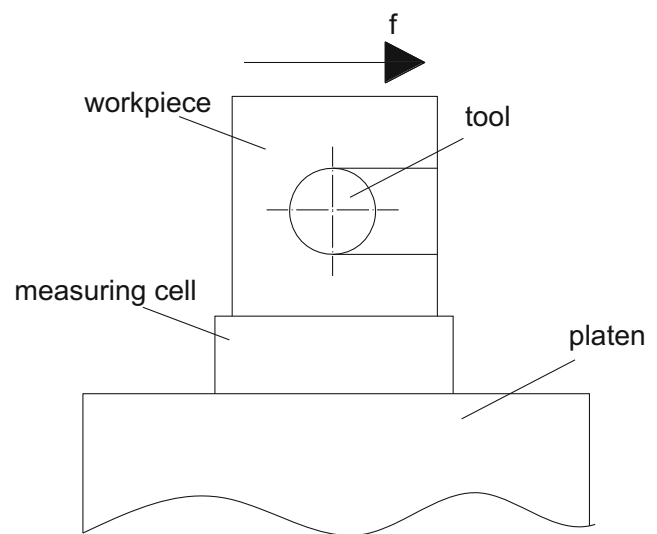
Another advantage is that the NURBS method is established by the data of the simulation. Therefore, it does not require experimental cutting force data, which is convenient.

In Sect. 6, an example of the cutting force research on the five-blade end milling cutter cutting the HT250 test piece is provided. However, the experimental cutting forces along the

feed speed and along the axial direction of the cutter exhibit obvious fluctuation. Two reasons are put forward to explain the obvious fluctuation of the experimental cutting force according to some literature, and these are also the reasons for the error between the cutting force simulation and experiment.

The first reason for the abovementioned fluctuation is the phenomenon of cutter runout in the cutting process. This will influence the entry and exit angle and the chip thickness in the cutting process [23, 24], which will result in the fluctuation of the experimental cutting force. This phenomenon was not included in the cutting force model based on NURBS and the FEM. This will influence the accuracy of cutting force prediction. In future work, the cutting force model will be improved by taking cutter runout into account.

The second reason is that the vibration of the spindle and workpiece will influence the cutting force [25, 26]. The stiffness along each dimension of the machine is different, which will cause different cutting force fluctuations in different dimensions. This cutting force is measured in the horizontal milling process. As Fig. 17 shows, the cutting force in the direction perpendicular to the feed speed is always perpendicular to the

Table 3 Comparison of the NURBS and FEM methods

	NURBS	FEM
The number of grids of the workpiece	512,342	9,124,180
The minimum size of the grids (mm)	0.0156441	0.022041
The rotation angle of the tool tip	1°	360°

Fig. 17 The diagram of clamping the workpiece in the horizontal milling process

platen. In this direction, the stiffness of the workpiece and the fixture is better. This would reduce the vibration amplitude in this direction. The vibration amplitude in the other direction will be stronger than the vibration amplitude perpendicular to the feed speed. The cutting force fluctuation in the other direction is larger as well. This point is proved in other studies. For example, Li proposed an algorithm to research the interaction between the cutting force and vibration and improved the precision of the cutting force simulation. In the literature, the vibration along the axial direction of the spindle was ignored because the stiffness of the spindle and workpiece is high in this direction [26]. The cutting force model based on NURBS and the FEM did not take the influence of the vibration into account. In future work, the interaction of the vibration and cutting force should be taken into account to improve the cutting force model.

8 Conclusions

A cutting force model has been developed using NURBS and the FEM. To predict the cutting force of the whole cutter, several cutting force simulations of the blade with different undeformed chip thicknesses and axial cutting depths should be accomplished first in this method. Based on these data, the tangential cutting force model, the radial cutting force model, and the axial cutting force model of the blade can be established by NURBS. With the motion model and the cutting force model of the blades, the cutting force of the whole cutter with different cutting parameters can be generated. This model has the following advantages:

1. The accuracy of the cutting force prediction is similar to the method of coefficient identification as Fig. 14 shows. In addition, the accuracy of the axial cutting force is improved compared with the method of cutting force coefficient identification.
2. The cutting force prediction method is more efficient than the FEM in the research of large diameter multi-blade face milling cutters. This method separates the whole cutter cutting force simulation into several single blade transient cutting force simulations to reduce the simulation time.
3. The NURBS method is established by the data of the simulation. Therefore, it does not require cutting force experimental cutting force data, which is convenient.

To improve the precision of the cutting force prediction model, the phenomenon of cutter runout and the vibration in the milling process will be researched in future work. The interaction between the vibration and cutting force will be included in the improved cutting force model, and a more accurate cutting force will be simulated in future work.

References

1. Brecher C, Esser M, Witt S (2009) Interaction of manufacturing process and machine tool. CIRP Ann Manuf Technol 58(2):588–607
2. Guo Q, Jiang Y, Zhao B (2016) Chatter modeling and stability lobes predicting for non-uniform helix tools. Int J Adv Manuf Technol 87(1–4):251–266
3. Altintas Y, Engin S, Budak E (1999) Analytical Stability Prediction and Design of Variable Pitch Cutters. J Manuf Sci Eng 121(2):173
4. Jáuregui JC, Reséndiz JR, Thenozhi S et al (2018) Frequency and time-frequency analysis of cutting force and vibration signals for tool condition monitoring, IEEE Access, 1-1
5. Anicic O, Jovic S, Stanojevic N et al (2018) Estimation of tool wear according to cutting forces during machining procedure. Sens Rev 38(2):176–180
6. Engin S, Altintas Y (2001) Mechanics and dynamics of general milling cutters: Part II: inserted cutters. Int J Mach Tool Manu 41(15):2195–2212
7. Liu XW, Cheng K, Webb D et al (2002) Improved dynamic cutting force model in peripheral milling. Part I: theoretical model and simulation. Int J Adv Manuf Technol 20(9):631–638
8. Tapoglou N, Antoniadis A (2012) 3-dimensional kinematics simulation of face milling. Measurement 45(6):1396–1405
9. Ghorbani H, Moetakef-Imani B (2015) Specific cutting force and cutting condition interaction modeling for round insert face milling operation, Int J Adv Manuf Technol, 1-11
10. Yoon MC, Kim YG (2004) Cutting dynamic force modelling of end milling operation. J Mater Process Technol 155–156(none):1383–1389
11. Jian Q (2018) Modeling of cutting force coefficients in cylindrical turning process based on power measurement, Int J Adv Manuf Technol
12. Bouacha K, Yallese MA, Mabrouki T (2010) Statistical analysis of surface roughness and cutting forces using response surface methodology in hard turning of AISI 52100 bearing steel with CBN tool. Int J Refract Met Hard Mater 28(3):349–361
13. Lalwani DI, Mehta NK, Jain PK (2008) Experimental investigations of cutting parameters influence on cutting forces and surface roughness in finish hard turning of MDN250 steel. J Mater Process Technol 206(1–3):167–179
14. Jain V, Raj T (2018) Prediction of cutting force by using ANFIS. Int J Syst Assur Eng Manag 1-10
15. Sharma VS, Dhiman S, Sehgal R (2008) Estimation of cutting forces and surface roughness for hard turning using neural networks. J Intell Manuf 19(4):473–483
16. Yao Q, Wu B, Luo M et al (2018) On-line cutting force coefficients identification for bull-end milling process with vibration. Measurement 125:243–253
17. Li Z, Li S, Zhou M, Study on dynamic simulation and cutting parameters optimization on complex cutting conditions milling process, International Conference on Intelligent Computation Technology and Automation. IEEE, pp.501–504, 2010
18. Yu G, Wang L, Wu J (2018) Prediction of chatter considering the effect of axial cutting depth on cutting force coefficients in end milling, Int J Adv Manuf Technol

19. Wan M, Zhang WH (2006) Calculations of chip thickness and cutting forces in flexible end milling. Int J Adv Manuf Technol 29(7–8):637–647

20. Domingo M, Rivas F, Perez J et al (2002) Computation of the RCS of complex bodies modeled using NURBS surfaces. IEEE Antenn Propag M 37(6):36–47

21. Shao C, Xiao L (2011) NURBS model for chaotic time series, International Conference on Computer Research and Development IEEE, pp.135–138

22. Wang B, Zhang Y, Liang J (2017) Simulation analyzing the influence of cutting HT250 by self-prepared Si3N4 insert at different feed rate, Materials Science and Engineering Conference Series Materials Science and Engineering Conference Series:012042

23. Kline WA, Devor RE (1983) The effect of runout on cutting geometry and forces in end milling. Int J Mach Tool Des Res 23(2–3): 123–140

24. Rivière-Lorphèvre E, Filippi E (2009) Mechanistic cutting force model parameters evaluation in milling taking cutter radial runout into account. Int J Adv Manuf Technol 45(1–2):8–15

25. Li XP, Zheng HQ, Wong YS (2000) An approach to theoretical modeling and simulation of face milling forces. J Manuf Process 2(4):225–240

26. Yang Y, Liu Q, Zhang B (2014) Three-dimensional chatter stability prediction of milling based on the linear and exponential cutting force model. Int J Adv Manuf Technol 72(9–12):1175–1185